



Synthesis and Characterization of $C_7H_{11}N_3O_2 \cdot 2HCl$ – A Histidinium Nlo Crystal

Helen Merina Albert¹ and C. Alosious Gonsago^{2*}

¹Department of Physics, Sathyabama University, Chennai-119, India

²Department of Physics, Mohamed Sathak College of Arts & Science, Chennai-119, India

*Corresponding author: C. Alosious Gonsago, Department of Physics, Mohamed Sathak College of Arts & Science, Chennai-119, India.

E-mail: dralosious@gmail.com

Received: 09-Sep-2019, Manuscript no: dpc-21-05-PreQc-22, Editor assigned: 13-Sep-2019, PreQC No: dpc-21-05-PreQc-22, Reviewed: 27-Sep-2019, QC No: dpc-21-05-PreQc-22, QI No: dpc-20-2291, Revised: 20-July-2022, Manuscript No: dpc-21-05-PreQc-22,

Published: 17-Aug-2022, DOI: 10.4172/0975-413X.14.8.01-07

ABSTRACT

L-histidinium methyl ester dihydrochloride $C_7H_{11}N_3O_2 \cdot 2HCl$, a semi-organic nonlinear crystal of L-histidine family was grown by slow evaporation method at room temperature. Single crystal X-ray diffraction, FT-IR and FT-Raman spectral studies were employed on the grown crystal. The UV spectral study was performed to find the optical transmittance of the grown compound in the visible and UV regions. Powder technique of Kurtz and Perry was employed to analyze the harmonic generation efficiency of the L-histidinium methyl ester dihydrochloride single crystal. The dielectric study was performed and the parameters such as dielectric loss and dielectric constant were studied. AC conductivity studies were performed. The mechanical behaviour of the grown crystal was studied using Vickers microhardness tester and the results are discussed.

Keywords: Single crystal, XRD, FT-Raman, Optical, Dielectric, Microhardness.

INTRODUCTION

There is an increase in demand of new types of crystals in technological applications due to the fact that bulk growth of semi-organic crystals in all three dimensions makes the crystal growth process easy and suitable for device fabrication [1]. The semiorganic crystals possess the strong NLO properties and chemical flexibility of organic materials and the physical sturdiness and excellent transmittance of inorganic materials [2–4]. At present, enhancement of nonlinear optical properties of semi-organic crystals plays the major role of investigation due to the added advantages of both organic and inorganic crystals. It is of great interest to grow semiorganic crystals using aminoacids with inorganic or metal complexes to enhance their physicochemical properties [5].

Amino acids are most suitable materials for nonlinear optical applications as it contains an asymmetric carbon atom which makes them optically active and also most of them except Glycine, crystallize in non-centrosymmetric space groups. Recently, numerous research works have been carried out to synthesize amino acid mixed organic and inorganic materials with improved chemical stability, optical, thermal, electrical, mechanical properties apt for nonlinear optical applications [6-8].

Semiorganic crystals of L-histidinium family such as L-histidinium monohydrochloride phosphate, L-histidinium cadmium chloride monohydrate and L-histidinium nitrates have been already reported by several authors and these materials were found to be nonlinear materials suitable for photonic applications [9–11]. Followed by the previous works, we have grown a semi-organic nonlinear optical material $C_7H_{11}N_3O_2 \cdot 2HCl$ (LHMED) for photonic industry applications. The preliminary structural studies of LHMED was already reported by Victor H. Vilchiz et al [12] and had been already identified as a promising material for optical applications. In this study, $C_7H_{11}N_3O_2 \cdot 2HCl$ crystals were synthesized and subjected to FTIR, FT-Raman spectral studies, optical studies, electrical and mechanical studies.

MATERIALS AND METHODS

The title compound $C_7H_{11}N_3O_2 \cdot 2HCl$ (AR grade) obtained from Sigma-Aldrich Company was purified by frequent recrystallization process in double distilled water before it was used for growth process. The growth experiment was performed in a constant temperature bath maintained at 32 °C. The salts obtained after recrystallization process were completely dissolved in double distilled water and subjected to continuous stirring using magnetic stirrer for about 6 hours. Once saturation of solution is achieved, it was filtered using micro-whatman filter paper to extract any unwanted impurities. The filtered solution was kept in a borosil beaker for further nucleation. The solution was then allowed for constant evaporation at room temperature. In order to sustain constant growth process without fungus formation, few drops

of H₂O₂ were added to the above supersaturated solution. Optically transparent LHMED single crystal of dimensions 15 mm × 7 mm × 3 mm was grown within a period of a month.

RESULTS AND DISCUSSION

Single crystal XRD

Crystal structure and lattice parameters of the as grown C₇H₁₁N₃O₂·2HCl were identified using single crystal X-ray diffraction technique. The crystallographic study has been carried out using Brukeraxs kappa apex2 CCD Diffractometer with MoK α radiation of wavelength 0.7107 Å at 293(3) K. A tiny crystal of dimensions 0.35 x 0.32 x 0.20 mm³ was used for experimental analysis. The XRD analysis confirms that the LHMED is crystallized in monoclinic form with space group of P21. The lattice parameters were calculated and the values are a=8.221(3) Å, b=7.108(3) Å, c=9.505(7) Å, V=553.681(5) Å³, $\alpha=\gamma=90^\circ$ and $\beta=94.56(5)^\circ$. The observed values are agreeing well with the reported values [12]. Molecular structure of C₇H₁₁N₃O₂·2HCl is depicted in Figure 1.

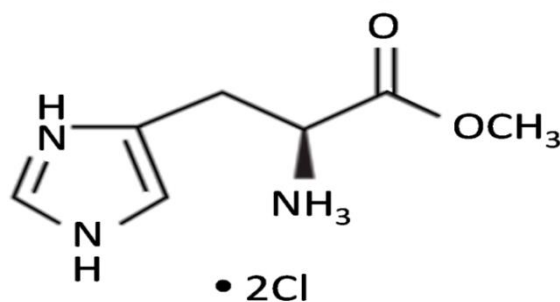


Figure 1: Molecular structure of C₇H₁₁N₃O₂·2HCl.

FT-IR and FT-Raman spectral studies

The FT-IR and FT-Raman spectral studies were carried out for the qualitative analysis and identification of compounds. FT-IR analysis was performed by KBr pellet technique in the frequency range 400–4000 cm⁻¹ using Perkin-Elmer spectrometer. FT-Raman study was performed using BRUKER RFS-27 Raman spectrometer in the frequency range 200–3500 cm⁻¹. Crystalline powders of C₇H₁₁N₃O₂·2HCl were used for the spectral analysis. The recorded FT-IR and FT-Raman spectra of LHMED are depicted in Figures 2 and 3. In the high frequency region of IR spectra, absorption band appearing at 3429 cm⁻¹ is due to the presence of hydrogen bond N-H stretching, characteristics of amino acids [13]. Their Raman equivalents are not observed since there is insufficient detector sensitivity in the region above 3300 cm⁻¹. The IR band at 3115 cm⁻¹ is due to the presence of NH₃⁺ group in the crystal and its Raman counterpart is observed at 3116 cm⁻¹. In the IR spectra, the aromatic C–H stretching and aliphatic C–H stretching modes are resolved at 3015 and 2886 cm⁻¹, whereas their Raman counterparts are observed at 3031 and 2889 cm⁻¹ respectively [14].

Multiple fine structures at the lower energy modes indicate strong hydrogen bonding interactions of NH₃⁺ groups with the COO⁻ group. The strongest IR band observed at 1759 cm⁻¹ indicates the presence of C=O stretching of carbonyl group and its Raman equivalent peak is resolved at 1756 cm⁻¹. The peak at 1625 cm⁻¹ in the IR spectra and 1626 cm⁻¹ in the Raman spectra is assigned to C=N stretching of imidazole ring. The aromatic C–C stretching vibrations are resolved at 1434 and 1430 cm⁻¹ in IR and Raman spectra respectively. The presence of strong IR band at 1291 cm⁻¹ and a weak Raman peak at 1279 cm⁻¹ is due to C–O stretching vibration of carbonyl group. The strong IR band at 1148 cm⁻¹ and a weak Raman counterpart at 1153 cm⁻¹ are due to the stretching vibration of C–O group of ester functionality. In the lower wavenumber region of IR spectra, the bands at 987, 868 and 622 cm⁻¹ are due to the ring asymmetric, symmetric stretching and plane deformation. Their Raman counterparts are observed at 989, 854 and 641 cm⁻¹ respectively. The assignments of various functional groups are detailed in Table 1.

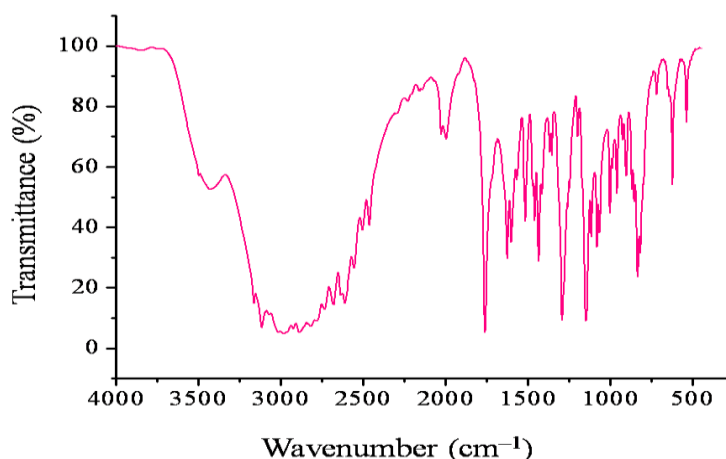


Figure 2: FT-IR spectrum of C₇H₁₁N₃O₂·2HCl.

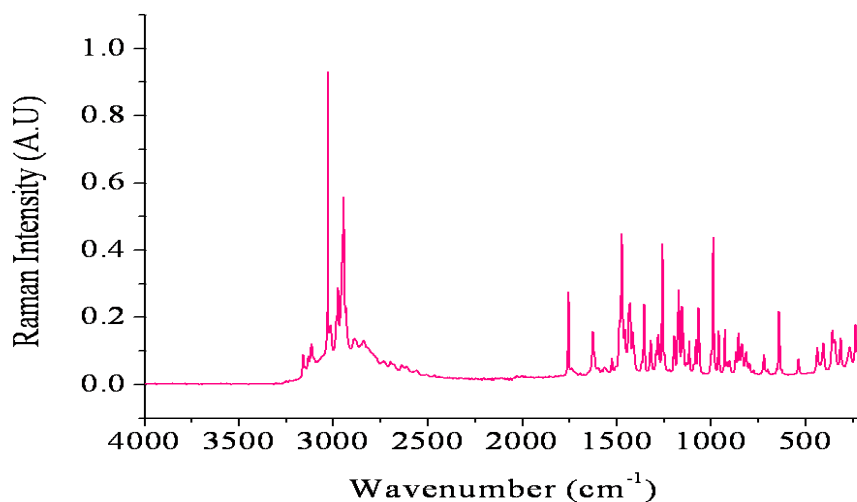


Figure 3: FT-Raman spectrum of C7H11N3O2.2HCl.

Table 1: FT-IR and FT-Raman spectral assignments of C7H11N3O2.2HCl.

Wavenumber (cm ⁻¹)		Assignment
IR	Raman	
3429	-	NH stretching
3162	3160	NH ₃ ⁺ stretching
3015	3031	Aromatic CH stretching
2920	2947	aliphatic CH ₂ stretching
2886	2889	Aliphatic C-H stretching
1759	1756	C=O Stretch of carbonyl group
1625	1626	C=N Stretching of imidazole ring
1600	-	Aromatic C=C Stretching
1568	1565	C=O asymmetric stretching
1515	1524	NH ₃ ⁺ Symmetric deformation
1458	1473	CH ₂ scissoring
1434	1430	C-C Stretching
1418	1414	C=O symmetric stretching
1291	1279	C-O stretching
1257	1257	CH ₃ stretching
1148	1153	C-O Stretching of Ester
1080	1081	C-N stretching
987	989	Ring asymmetric stretching
868	854	Ring symmetric
833	836	C-C-O stretch
718	720	CH ₂ rocking
622	641	Ring deformation
537	538	Torsional oscillation of NH ₃ ⁺

Optical absorption study

In order to find the optical transmittance of LHMED crystal, optical absorption study was carried out using the instrument Varian Carry-5E UV-Vis spectrophotometer in the wavelength region 200-1000 nm. The recorded optical absorption spectrum of LHMED is depicted in Fig.4. The LHMED crystal shows negligible absorption in the visible and near UV region which facilitate it to be a possible material for nonlinear and optoelectronic applications [15]. The absorption spectrum shows that the transparency of the crystal widen up to the wavelength 230 nm which represents the lower cut-off wavelength or fundamental absorption of the crystal. The low absorption range or wide transparency window between 230 nm and 1000 nm is adequate for the second harmonic generation of light from the C7H11N3O2.2HCl crystal using the Nd: YAG laser.

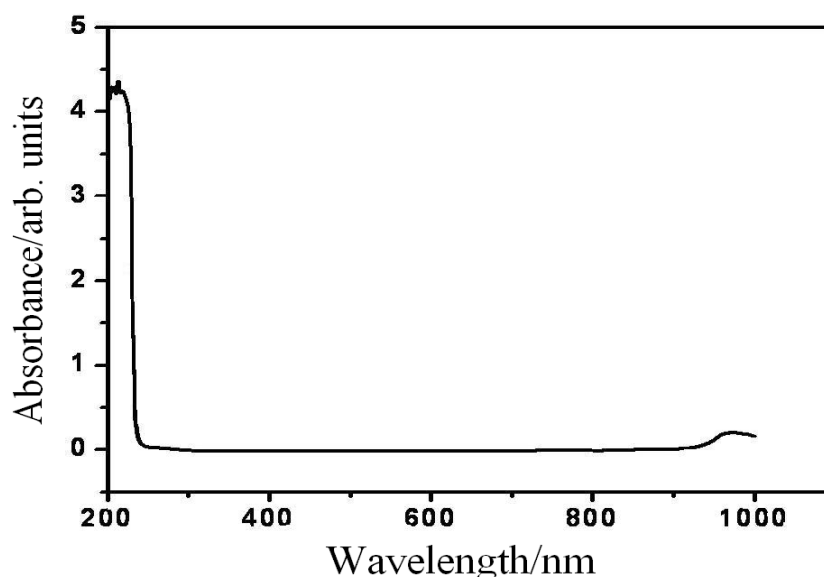


Figure 4: Optical transmittance spectrum of $C_7H_{11}N_3O_2 \cdot 2HCl$ crystal.

Second harmonic generation

Kurtz and Perry powder technique was followed to find the second harmonic generation of $C_7H_{11}N_3O_2 \cdot 2HCl$ crystal [16]. A Q-switched Nd: YAG laser generating the fundamental wavelength 1064nm, pulse width 8 ns having the repetition rate of 10 Hz was used for this purpose. It has been observed that the LHMED sample converts the input radiation of wavelength 1064 nm in to green radiation of wavelength 532 nm. The conversion efficiency of the $C_7H_{11}N_3O_2 \cdot 2HCl$ is compared with the microcrystalline KDP sample and it has been observed that output from the $C_7H_{11}N_3O_2 \cdot 2HCl$ sample is 53 mV and for the reference KDP sample is 33 mV.

Dielectric studies

The dielectric constant of $C_7H_{11}N_3O_2 \cdot 2HCl$ sample was measured in the frequency range from 50 Hz to 5 MHz for the temperature range 313–373 K. The variation of dielectric constant with log frequency at different temperatures is shown in Figure 5. It is observed that the dielectric constant is higher at lower frequencies. The dielectric constant decreases exponentially with increasing frequency and reaches a minimum value at higher frequencies. This can be understood on the basis of polarization mechanism. The electronic exchange between ions in the crystal gives local displacement of electrons in the direction of the applied electric field which gives polarization. Generally, at low frequencies the dielectric constant of the material is due to the contribution of electronic, ionic, dipolar and space charge polarizations. As the frequency increases, space charge cannot follow the external field and hence polarization decreases, giving rise to smaller values of dielectric constant. Further, it has been observed that the dielectric constant decreases with increase in temperatures.

The variation of dielectric loss with log frequency at different temperatures is shown in Figure 6. As the frequency increases, the dielectric loss decreases and at higher frequencies it almost becomes zero. The dielectric constant and dielectric loss show similar responses with frequencies at all temperatures. The low value of dielectric loss at high frequency implies that the crystal possesses better optical quality with lesser defects and this parameter is crucial for NLO materials in their application.

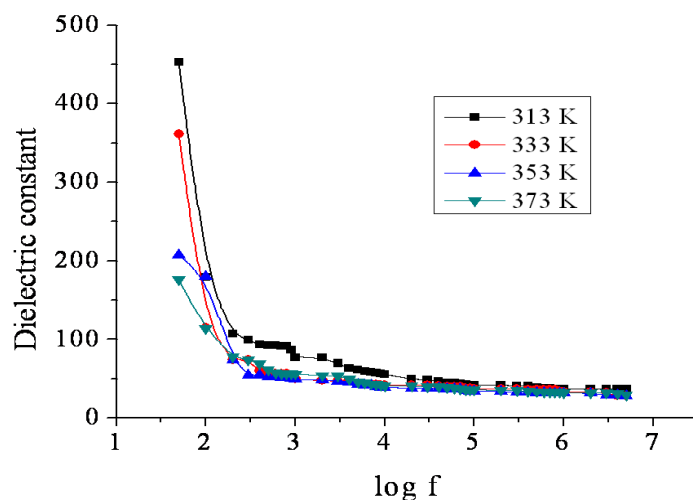


Figure 5: Variation of dielectric constant with log frequency.

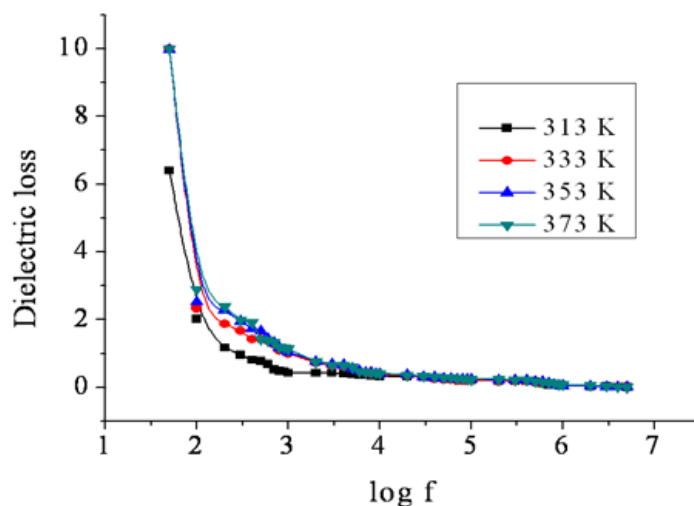


Figure 6: Variation of dielectric loss with log frequency.

AC Conductivity study

Electrical conductivity is an impurity controlled process in the low temperature region and a defect-controlled process in the high temperature region. The AC conductivity (σ_{ac}) of the LHMED can be found using the relation $\sigma_{ac} = 2\pi f \epsilon_0 \epsilon_r \tan \delta$, where f is the frequency of the alternating current, ϵ_0 is the permittivity of free space, ϵ_r is the dielectric constant and $\tan \delta$ is the dielectric loss. The variations of AC conductivity with different temperatures for $C_7H_{11}N_3O_2 \cdot 2HCl$ samples are shown in the Figure 7. It has been observed that the values of AC conductivity increases with increase in temperature for the samples. When the sample is subjected to high temperature, there is a possibility of weakening of the hydrogen bonds and more and more defects are created. This may results in increase in electrical conduction in the sample.

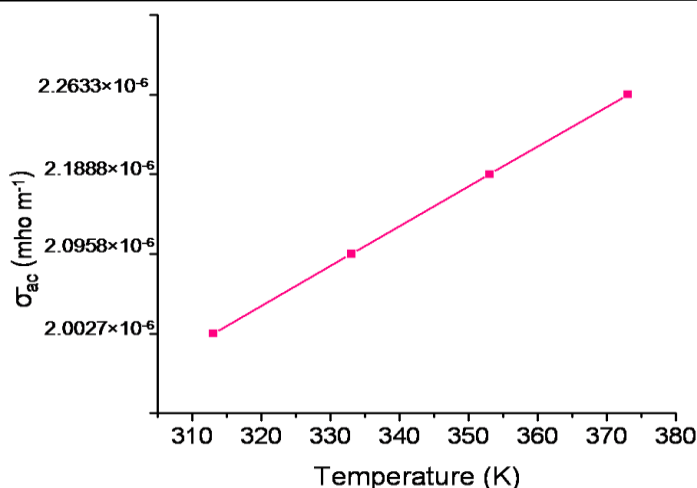


Figure 7: Variation of AC conductivity with temperature.

Microhardness Analysis

Mechanical behaviour of $C_7H_{11}N_3O_2 \cdot 2HCl$ crystal was analyzed by measuring the microhardness number with different loads. The hardness of an ideal crystal should be independent of the applied load. But in practice, due to normal indentation size effect the load dependence is observed. In present study, static indentations were made on the $C_7H_{11}N_3O_2 \cdot 2HCl$ crystal for different loads from 10 to 50 g at 32°C with a constant indentation time of 15 s. Due to the formation of possible cracks on the crystal surface at higher loads, the maximum applied load was limited to 50 g. The hardness number H_v of the LHMED was calculated using the formula $H_v = 1.8544 P/d^2$ kg/mm² where, P is the applied load in kg and d is average diagonal length of the indentation in mm. A graph is drawn between hardness number (H_v) and applied load (P) and is depicted in Figure 8.

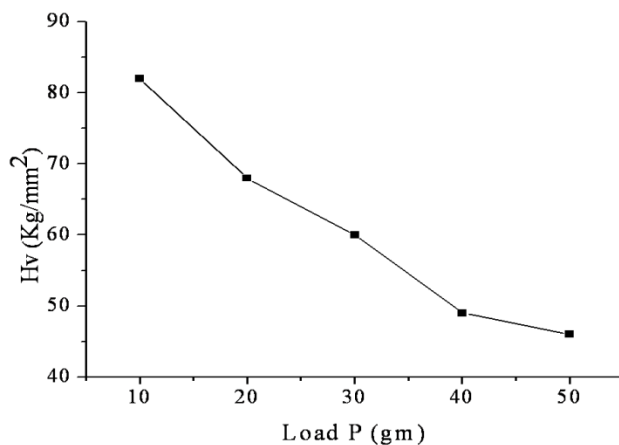


Figure 9: Variation of hardness number (H_v) with applied load (P).

It has been observed that the hardness of LHMED crystal decreases with increasing load, which is attributed to normal indentation size effect. By employing least square fit method, the value of work hardening coefficient 'n' was estimated from the plot of $\log P$ versus $\log d$ (Figure 10). According to on its CH, for $1.0 \leq n \leq 1.6$ the material is regarded as hard material and $n > 1.6$ for soft materials [17]. In the present work, the value of n is calculated as 1.46 and thus confirming that LHMED is a hard material.

CONCLUSION

$C_7H_{11}N_3O_2 \cdot 2HCl$ single crystal was grown from aqueous solution by slow solvent evaporation method at room temperature. X-ray diffraction study shows that the $C_7H_{11}N_3O_2 \cdot 2HCl$ crystal belongs to monoclinic system with the space group P_{21} . Structure $C_7H_{11}N_3O_2 \cdot 2HCl$ was elucidated by FT-IR and FT-Raman spectroscopy. The optical absorption study shows that the grown crystal is free from any absorption in the UV and visible region and thus confirms the suitability of the crystal for photonic applications. Microhardness study reveals that the hardness number H_v decreases with increasing load and also LHMED belongs to the category of hard materials.

The SHG test reveals that the conversion efficiency of C₇H₁₁N₃O₂.2HCl was observed to be 1.6 times more than that of standard KDP sample. The low value of dielectric constant and dielectric loss combined with the relatively high SHG conversion efficiency make it a promising material for photonic applications.

REFERENCES

- [1] Arockia AS, Leo RA, *J Mater Sci Mater Elect*, 2017, 28: p. 10893–1090.
- [2] Mahadevan M, Sankar PK, Vinitha G, *et al.*, *Opt Laser Tech*, 2017, 92: p. 168-172.
- [3] Surekha R, Thilagavathy SR, Sagayaraj P, *Optik*, 2014, 125: p. 934-938.
- [4] Kumar S, Paulraj CR, Ramasamy P, *Spect Chim Acta A*, 2015, 151: p. 432-437.
- [5] Chinnappan CP, Selvaraj A, Stalin JP, *et al.*, *Optik*, 2016, 127: p. 110-115.
- [6] Marcy HO, Rosker MJ, Warren LF, *et al.*, *Opt Lett*, 1995, 20: p. 252–254.
- [7] Chinnappan CP, Selvaraj A, Stalin JP, *Optik*, 2015, 126: p. 5517-5521.
- [8] Edwin SG, Manimaran D, Hubert JI, *et al.* *Mater Today*, 2015, 2: p. 987-991.
- [9] Anuradha GV, *Optik*, 2015, 126: P. 4743-4746.
- [10] Chandrasekaran P, Ilayabharathy P, Maadeswaran P, *et al.*, *Opt Comm*, 2012, 285: p. 2096-2100.
- [11] Petrosyan HA, Karapetyan HA, Petrosyan AM, *J Mol Struct*, 2006, 794: p. 160–167.
- [12] Vilchiz VH, Norman RE, Chang SC, *Acta Cryst*, 1996, C51: p. 696–698.
- [13] Rao CNR, *Chemical Application of Infrared Spectroscopy*, Academic Press, New York, 1963.
- [14] Bellamy LJ, *The infrared spectra of complex molecules*, Wiley, New York, 1975.
- [15] Alosious GC, Helen MA, Karthikeyan J, *et al.*, *Mater Res Bull*, 2012, 47: p. 1648–1652.
- [16] Kurtz SK, Perry TT, *J Appl Phys*, 1968, 39: p. 3798–3813.
- [17] Onitsch EM, *Mikroskopie*, 1956, 95: p. 12–14.